

**Original Paper, Endocrine.**

## **Utility of $^{99m}\text{Tc}$ -MIBI Single Photon-Emission Computed Tomography/Computed Tomography in Pre-Surgical Characterization of Thyroid Follicular Neoplasm.**

**Mostafa, NM<sup>1</sup>. Rezk, Kh<sup>2</sup>. Khalifa, W<sup>3</sup>. Ali, W<sup>4</sup>. Sherif, M<sup>5</sup>. Mohamadien, N<sup>1</sup>.**

*<sup>1</sup>Nuclear Medicine Unit, Department of Clinical Oncology and Nuclear Medicine, Faculty of Medicine. <sup>2</sup>Department of Surgical Oncology, South Egypt Cancer Institute. <sup>3</sup>Department of Internal Medicine, Faculty of Medicine. <sup>4</sup>Department of Diagnostic and Interventional Radiology, Faculty of Medicine, <sup>5</sup>Department of Pathology, Faculty of Medicine, Assiut University, Egypt*

### **ABSTRACT:**

**Background:**  $^{99m}\text{Tc}$ -Sestamibi (MIBI) thyroid scintigraphy is an increasingly used non-invasive imaging tool for evaluation of thyroid nodules. Yet the results are heterogeneous. The aim of this study was to evaluate the utility of  $^{99m}\text{Tc}$ -MIBI for differentiating benign from malignant thyroid nodules with a cytological reading of follicular neoplasm. **Patients and Methods:** Twenty-one patients were prospectively imaged by  $^{99m}\text{Tc}$ -Pertechnetate and MIBI scans with addition of SPECT/CT. Images were visually interpreted using a scoring system: 0; no, 1; faint, 2; isointense and 3; intense uptake. Pattern of tracer washout in

delayed images was compared to early images; decreased, constant or increased uptake. Quantitative analysis was done to calculate washout and retention indices for planar (WOI-P and RI-P) and SPECT/CT images (WOI-S and RI-S). Inter-reader agreement was conducted for visual analysis. Histopathology and radiologic follow up were used as the gold standard. **Results:** Sixteen and 5 nodules proved benign and malignant respectively. The majority of nodules (63%) were hypofunctioning. Delayed MIBI scan scoring proved superior to the early one with 100% NPV.

Pattern of washout in SPECT/CT images had significantly higher specificity, PPV, NPV, and accuracy than that of the planar images ( $P=0.003$ ), yet both had the same sensitivity (80 %). I-P had a significant AUC of 0.850 ( $P= 0.021$ ) and a cut-off value of  $\geq -114$  gives 100% sensitivity and specificity, additionally it was the only the significant predictor factor for malignancy ( $P=0.02$ ). Inter-observer kappa agreement

was excellent for early planar and delayed SPECT/CT (95%CI: 0.00-0.133,  $p<0.01$  and 95%CI: 1.00-1.00,  $p<0.0$  respectively).

**Conclusion:** The visual scoring system yields a high sensitivity and NPV, yet it has a low specificity. Addition of SPECT/CT improves the diagnostic accuracy of the washout pattern in the delayed images. RI-P was the only significant predictor factor for malignancy.

**Key Words:** Sestamibi, MIBI washout, thyroid nodules, scoring system, semi quantitative parameters.

---

**Corresponding Author:** Mohamadien, N.

**E-mail:** [nadia.khalifa@med.aun.edu.eg](mailto:nadia.khalifa@med.aun.edu.eg).

## INTRODUCTION:

Thyroid nodules are a common clinical problem, representing about 5% in women and 1% in men in iodine-sufficient areas of the world reaching up to 68% in randomly selected individuals, yet only 5% are malignant <sup>(1, 2)</sup>. The diagnostic approach to thyroid nodules is usually based on clinical examination, laboratory tests, ultrasound (US), and scintigraphy; followed by the well-established complementary procedure of fine-needle aspiration cytology (FNAC) in case of suspicious nodules <sup>(3)</sup>. US is the first line imaging examination; it can help in differentiating benign from malignant thyroid nodules, but individual US features may be of limited value <sup>(4)</sup>.

FNAC is a rapid, cost effective and available diagnostic modality <sup>(5)</sup> mainly used to identify patients who actually require surgery, thus reducing the number of unnecessary thyroidectomies and its complications <sup>(6)</sup>.

Generally, FNAC is reported as non-diagnostic, benign, atypia of undetermined significance or follicular lesion of undetermined significance, follicular neoplasm or suspicious for follicular neoplasm, suspicious for malignancy, and malignant <sup>(1)</sup>. Yet it has limitations in that both false-positive and false-negative results can occur <sup>(7)</sup>.

Moreover, thyroid nodules with a follicular growth pattern on FNAC involve a wide spectrum of lesions, ranged from benign (hyperplastic nodules and follicular adenoma) to malignant (follicular carcinoma and follicular variant of papillary thyroid carcinoma) lesions, which requires surgical excision for definitive histopathological diagnosis<sup>(8)</sup>.

Thyroid scintigraphy with  $^{123}\text{I}$  or  $^{99\text{m}}\text{Tc}$ -pertechnetate reflects the metabolic rate of thyroid cells and considered as a well-established tool for ruling out malignancy in hyperfunctioning (i.e. hot) nodules, while  $^{99\text{m}}\text{Tc}$ -methoxyisobutylisonitrile ( $^{99\text{m}}\text{Tc}$ -MIBI) thyroid scanning reflects the actively functioning mitochondria and therefore cellular oxidative metabolism and has been proposed for differentiating benign from malignant hypofunctioning (i.e. cold) thyroid nodules with a high negative predictive value of up to 100%<sup>(3, 9-11)</sup>. Several studies have evaluated the potential role of  $^{99\text{m}}\text{Tc}$ -MIBI scanning for predicting or excluding malignancy in hypofunctioning thyroid nodules but the results are heterogeneous<sup>(12, 13)</sup>.

The aim of this study was to evaluate the role of  $^{99\text{m}}\text{Tc}$ -MIBI thyroid scintigraphy in differentiating benign from malignant thyroid nodules in patients with a cytological reading of follicular neoplasm.

## **MATERIALS AND METHODS:**

Following approval of our institutional review board with an informed written consent obtained from each patient, we prospectively studied 21 patients with proven or suspicious cytology of follicular neoplasm, normal thyrotropin (TSH) level, hypo or isofunctioning nodule(s) on  $^{99\text{m}}\text{Tc}$ -Pertechnetate thyroid scintigraphy, and thyroid nodule(s) >1 cm in maximum diameter on US. We excluded patients less than 18 years old, those with history of thyroid surgery or radiotherapy, diffuse thyroid swellings, hyper or hypothyroidism patients, and pregnant females.

Complete medical history was obtained from all patients and all of them underwent clinical examination, measurement of TSH level, thyroid US (considering nodule diameters, structure, echogenicity, vascularity, presence or absence of irregular margins, presence or absence of microcalcifications), and nuclear medicine studies ( $^{99\text{m}}\text{Tc}$ -pertechnetate thyroid scintigraphy and  $^{99\text{m}}\text{Tc}$ -MIBI scintigraphy).

### **$^{99\text{m}}\text{Tc}$ -pertechnetate thyroid scintigraphy:**

Thyroid scintigraphy was obtained by using dual-head SPECT/CT gamma camera (Symbia T, Siemens Healthcare) fitted with low energy all-purpose parallel whole (LEAP) collimators, using a 20 % energy window set at 140 keV.

Planar anterior images of the neck were obtained 15–20 minutes after intravenous injection of 74–111 MBq (2-3 mCi)  $^{99m}\text{Tc}$ -pertechnetate using magnification of 1, matrix size of  $256 \times 256$ , and frame time of 100 K counts.

**$^{99m}\text{Tc}$ -MIBI scanning protocol:** Planar images were obtained approximately at 30 min (Early images) and 90-120 min (Delayed images) after intravenous injection of 740 MBq (20 mCi)  $^{99m}\text{Tc}$  -MIBI using the same gamma camera used in  $^{99m}\text{Tc}$  pertechnetate scan.

Imaging obtained in the supine position. Immediately after planar imaging at both time points; with the patient still in the same supine position; SPECT acquisition was obtained in a step-and-shoot mode (25s /stop), a total of 64 frames were acquired in a non-circular 360-degree arc and a matrix size of  $128 \times 128$ . Then a low dose CT was acquired for anatomical localization and attenuation correction. The used CT parameters were; tube voltage 130kV, tube current 80 mA and slice thickness of 1 mm, transverse, sagittal, and coronal slices were generated. Finally, SPECT images were coregistered and fused with CT images.

**Qualitative analysis for pertechnetate and MIBI scans:** Tracer uptake at both pertechnetate and MIBI scans was reported visually by two experienced nuclear medicine physicians independently and blinded to the clinical data. To measure interobserver agreement, the disagreed readings were discussed by the two physicians then a consensus reading was obtained.

Visual analysis was done by scoring method where score 0 means no uptake, score 1; faint uptake, score 2; isointense uptake and score 3; intense uptake. Score 0 and 1 considered negative while score 2 and 3 considered positive for tracer uptake.

**Semi-quantitative analysis for planar and SPECT/CT MIBI scans:** Semi-quantitative analysis was performed for both early planar and SPECT/CT images by drawing a region of interest (ROI) and a volume of interest (VOI) respectively over the perimeter of the thyroid nodule, then copied into the corresponding site in the contralateral normal thyroid lobe as well as to the outside of thyroid bed, e.g. right superior region of the patient's thorax (for background correction).

ROI was then copied into the delayed planar images, while nearly the same sized VOI was re-drawn in the delayed SPECT/CT images. The mean count in each ROI/VOI was determined to calculate both early ratio (ER) and delayed ratio (DR) for planar (ER-P and DR-P) and SPECT/CT (ER-S and DR-S) images via dividing the nodule counts by the normal tissue counts after background correction. The early and delayed uptake results for planar (EUR-P and DUR-P) and SPECT/CT images (EUR-S and DUR-S) were calculated by subtracting the mean background count from the mean nodule count. Thereafter, the washout index (WOI) for both planar (WOI-P) and SPECT/CT (WOI-S) images was calculated using the formula:  $WOI-P = [(DUR-P/EUR-P \times 100) - 100]$  and  $WOI-S = [(DUR-S/EUR-S \times 100) - 100]$  respectively. In addition, the retention index (RI) for both planar (RI-P) and SPECT/CT (RI-S) was also calculated using the formula:  $RI-P = (DR-P - ER-P) \times 100/ER-P$  and  $RI-S = (DR-S - ER-S) \times 100/ER-S$  respectively.

**Fine needle aspiration cytology:** Fine needle aspiration was operated by a Board certified experienced cytopathologist, using 22-gauge needle attached to 5ml plastic syringe under ultra-sonographic guidance. Two to three passes were done from the nodule for conventional smear cytology.

The aspirated material was expelled and smeared onto uncharged slides and stained by May-Grunwald-Giemsa stain for on site evaluation to check the adequacy of cytologic material. Presence of well-preserved 6 groups of follicular cells each containing at least 10 cells were considered adequate<sup>(14)</sup>. Another slide was prepared for Papanicolaou staining. Cytologic diagnosis of follicular neoplasm was performed on according to the recent cytologic criteria of The Bethesda system, 2018<sup>(15)</sup>.

**Reference standard:** Histopathological diagnosis was considered the gold standard for most of the study population apart from four cases where long term follow-up and radiologic imaging's were considered as the gold standard.

**Statistical analysis:** Data were analyzed using SPSS version 20.0 software (Statistical Package for the Social Sciences, IBM Inc., Armonk, New York, USA). Parametric variables were expressed as the mean +/- SD. For nonparametric variables we used median and IQR. Mann-Whitney-U test and Independent sample t-test were used to compare the medians and means respectively. Sensitivity, specificity, diagnostic accuracy, positive and negative predictive values were calculated for <sup>99m</sup>Tc-MIBI.

Receiver operating characteristic (ROC) analysis was performed to determine the best cutoff value above which malignant thyroid nodules could be detected by the used parameters. Spearman's rank correlation coefficient analysis was used to assess the correlation between variables, where the degree of correlation was considered as negligible (0.00–<0.10), weak (0.1–0.39), moderate (0.40–0.69), strong (0.70–0.89) or very strong (0.90–1.00). Regression analysis conducted to assess the independent variables for malignancy prediction. A significant P value was considered when it is less than 0.05.

## RESULTS:

**Patients and thyroid nodules:** Over a period of 36 months; Twenty-One patients diagnosed as follicular neoplasm by FNAC; (2 males and 19 females. Mean age;  $38.8 \pm 13$  years, range; 23–62 years) were enrolled in this prospective study. The mean size of the nodules was  $3.37 \pm 1.2$  cm (range: 2– 6.8 cm). No significant difference in nodule size was found between benign and malignant thyroid nodules ( $3.3 \pm 1$  for benign nodules Vs,  $3.7 \pm 1.9$  for malignant ones,  $P= 0.697$ ).

Patients with benign nodules were older than those with malignant ones (mean age was  $40 \pm 13.5$  years for patients with benign nodules and  $35 \pm 12.5$  years for those with

malignant ones,  $P=0.468$ ). Majority of patients (16/21) had solitary nodule and only 5/21 patients had a multinodular goiter.

In the  $^{99m}\text{Tc}$ -pertechnetate scintigraphy, 12 (57.2%) nodules were hypofunctioning, 7 (33.3%) were isofunctioning, and 2 patients didn't undergo  $^{99m}\text{Tc}$ - scan (9.5%).

The mean TSH value was  $1.8 \pm 1$   $\mu\text{IU}$  (range 0.5–4.3  $\mu\text{IU}$ ). Characteristics of the thyroid nodules were summarized in **Table (1)**.

### **FNAC and histopathological results:**

According to Bethesda system classification, all nodules were reported as follicular neoplasm (category IV). Only 17/21 patients underwent surgery (total thyroidectomy in 16/17 and hemi-thyroidectomy in one case), while the remaining 4 patients refused surgery and were followed up clinically and by US to reach a final diagnosis.

The histopathological examination revealed 12 (70.6%) benign (2 hurthle adenomas, 1 hyperplastic nodule, and 9 follicular adenomas, (**Figure 1**) and 5 (29.4 %) malignant nodules. From the malignant neoplasm (5), 2/5 were follicular variant of papillary thyroid carcinoma (**Figure 2**), 2/5 were minimally invasive follicular carcinoma, and the last one (1/5) was poorly differentiated thyroid carcinoma. Patients who refused surgery their follow up revealed benign nature of the nodule.

**Table (1):** Nodules characteristics in 21 patients of studied group.

Characteristic	Final diagnosis		P
	Benign 16 (76.2%)	Malignant 5 (23.8%)	
Mean age (years $\pm$ SD)	40 $\pm$ 13.5	35 $\pm$ 12.5	0.468**
Size of nodule (cm) • Mean $\pm$ SD	3.3 $\pm$ 1	3.7 $\pm$ 1.9	0.697**
Laterality: • Right • Left	9 (65.2%) 7 (43.8%)	5 (100%) 0	0.070*
Number: • Solitary • MNG	12 (75%) 4 (25%)	4 (80%) 1 (20%)	0.819*
Echogenicity: • Hypoechoic • Isoechoic • Hyperechoic • Heterogenous	7 (43.8%) 7 (43.8%) 1 (6.2%) 1 (6.2%)	1 (20%) 1 (20%) 0 3 (60%)	0.065*
Margin: • Well defined • Ill-defined • Not reported	10 (62.5%) 0 6 (37.5%)	3 (60%) 1 (20%) 1 (20%)	0.169*
Shape: • Ovoid • Wider than tall • Not reported	4 (25%) 1 (6.2%) 11 (68.8%)	2 (40%) 0 3 (60%)	0.720*
Calcification: • Present • Absent	2 (12.5%) 14 (87.5%)	1 (20%) 4 (80%)	0.676*
Degeneration/cystic changes: • Present • Absent	6 (37.5%) 10 (62.5%)	2 (40%) 3 (60%)	0.920*

\*Chi-square test, \*\*Independent sample t-test.

**Qualitative evaluation:** The two physicians agreed in the scoring of 18/19  $^{99m}\text{Tc}$  thyroid scans, 21 early and 18 delayed planar MIBI scans with inter-observer kappa agreement of 0.905, 1, and 0.789 respectively (95%CI: 0.00-0.133 with  $p < 0.01$  for all). The agreement value for SPECT/CT images was 1 (95%CI: 1.00-1.00 with  $p < 0.01$ ).

**Visual analysis of  $^{99m}\text{Tc}$ -pertechnetate thyroid scintigraphy:**

Nineteen out of the study population underwent thyroid scintigraphy; 12 of them had hypofunctioning nodules (2 were score 0 and 10 were score 1) while the other 7 cases had isofunctioning nodules (score 2), and none of the nodules were hyperfunctioning. Only 3 out of the hypofunctioning nodules revealed malignancy in histopathology and 6 out of the isofunctioning ones revealed benign nature.

**Visual analysis of early MIBI**

**images:** Among the benign nodules; 1/16 had score 1, 6/16 had score 2, and the remaining 9/16 nodules had score 3. Among the malignant nodules; 1/5 nodule had score 1, 2/5 nodules had score 2, and the remaining 2/5 nodules had score 3.

**Visual analysis of delayed planar**

**MIBI images:** Among the benign nodules, 5 had score 1, 5 had scored 2, and the remaining 6 nodules had score 3.

Out of the malignant nodules, 4 nodules had score 2 and 1 nodule had score 3.

The visual scoring had a high sensitivity in thyroid scintigraphy as well as in both MIBI images but low specificity in all of them especially the early MIBI images, the scoring of the visual analysis and its diagnostic performance were illustrated at *Tables (2, 3)*.

**Visual analysis of the pattern of washout for both planar and**

**SPECT/CT MIBI images:** Regarding the pattern of washout: complete tracer washout was considered as negative for malignancy, while both of constant and increased tracer uptakes were considered as suspicious for malignancy.

**Pattern of washout in planar**

**imaging:** Out of the benign nodules, 12/16 showed complete washout, 3/16 showed constant uptake, and only 1 nodule showed increased uptake (tracer retention).



Out of the malignant nodules, only 1 exhibited complete washout and the remaining 4 nodules revealed constant uptake. Twelve cases were true negative, 4 cases were true positive, 1 case was false negative, and 4 cases were false positive giving 80 % sensitivity and 75% specificity, accuracy of 76.2%, PPV of 50 %, and NPV of 92.3 % (P=0.040).

**Pattern of washout in SPECT/CT imaging:** The pattern of washout successfully diagnosed and ruled out malignancy in 4 and 13 lesions respectively, with 1 false negative case and 3 false positive cases giving sensitivity of 80 %, 81.2% specificity, 80% PPV, 92.7% NPV, and accuracy of 80.95% (P=0.003).

**Table (2):** Scoring and washout pattern of the nodules in 21 patients of studied group.

Variable	Benign nodules	Malignant nodules	P
<b><sup>99m</sup>Tc thyroid scan scoring:</b>			
• Score 0	1 (6.7%)	1 (25%)	0.581*
• Score 1	8 (53.3 %)	2 (50%)	
• Score 2	6 (40%)	1 (25%)	
<b>MIBI planar scoring:</b>			
• <b>Early:</b>			0.620*
○ Score 0	0	0	
○ Score 1	1 (6.2%)	1 (20%)	
○ Score 2	6 (37.5%)	2 (40%)	
○ Score 3	9 (56.2%)	2 (40%)	
• <b>Delayed:</b>			0.134*
○ Score 0	0	0	
○ Score 1	5 (31.2%)	0	
○ Score 2	5 (31.2%)	4 (80%)	
○ Score 3	6 (37.5%)	1 (20%)	
<b>Pattern of washout in planar images:</b>			
• Complete washout	12 (75%)	1 (20%)	0.040*
• Constant uptake	3 (18.8%)	4 (80%)	
• Increased uptake (retention)	1 (6.2%)	0	
<b>Pattern of washout in SPECT/CT images:</b>			
• Complete washout	13 (81.2%)	1 (20%)	0.003*
• Constant uptake	1 (6.2%)	4 (80%)	
• Increased uptake (retention)	2(12.4%)	0	

\*Chi-square test.

**Table (3):** Diagnostic performance of the scoring system and washout pattern in 21 patients with thyroid nodules.

Variable	Sensitivity %	Specificity %	PPV %	NPV %	Accuracy %	P
<sup>99m</sup> Tc thyroid scan	75	40	14.3	28.5	42.8	0.581
Early planar MIBI scan scoring	80	6.2	78.9	50	23.8	0.620
Delayed planar MIBI scan scoring	100	31.2	31.3	100	47.6	0.134
Pattern of washout in planar images	80	75	50	92.3	76.2	0.040
Pattern of washout in SPECT/CT images	80	81.2	80	92.7	80.95	0.003

**Quantitative planar and SPECT/CT analysis:**

Regarding quantitative analysis; the median values of WOI-P and WOI-S for benign nodules were insignificantly lower than those for the malignant ones (P=0.457 and 0.160, respectively).

The mean RI-P of benign nodules was significantly lower than that of malignant ones (31.6± 63.2 vs. 42.9± 41, P=0.024), while the median RI-S of benign nodules was insignificantly higher than that of the malignant ones (*Table 4*).

**Table (4):** Quantitative MIBI parameters in 21 patients with thyroid nodules.

Parameter	Benign nodules Median (IQR)	Malignant nodules Median (IQR)	P-value
WOI-P	-75.9(38.5)	-88.5(29.8)	0.457#
WOI-S	-60.7(161.7)	-71.8(30.9)	0.160#
RI-P (Mean± SD)	31.6± 63.2	42.9± 41	0.024**
RI-S	99.7(361)	-4.9(1740)	0.283#

#Mann whiteny U test, \*\* Independent sample t-test.

ROC analysis was conducted over the quantitative parameters to determine which of them better to rule out malignancy, only RI of planar images was the significant one

(AUC of 0.850 and P-value of 0.021). (Figure 3 & Table 5). In regression analysis, RI-P was the only significant predictor factor (p=0.02).

**Table (5):** AUCs of the quantitative parameters in 21 patients with thyroid nodules.

Variable	AUC (95% CI)	Cut-off	Sensitivity	Specificity	P-value
WOI-P	0.613 (0.354-0.871)	≥ -206.3	93.8	100	0.457
WOI-S	0.713 (0.491-0.934)	≥ -132.7	93.8	100	0.160
RI-P	0.850 (0.683-1.00)	≥ -114	100	100	0.021
RI-S	0.663 (0.383-0.942)	≥ -174	93.8	80	0.283

**Correlation of MIBI parameters, age, TSH, and nodule size:** All quantitative MIBI parameters were insignificantly positively correlated with age. WOI-P and RI-S were insignificantly positively correlated with TSH level, while WOI-S and RI-P were insignificantly negatively correlated with it. Insignificant positive

correlation was found between nodule size and WOI-P (r=0.202, with p=0.393), while insignificant negative correlation was found between it and each of age, TSH, WOI-S, RI-P, and RI-S (r=-0.264, -0.140, -0.193, -0.276, and -0.413 with P=0.616, 0.555, 0.414, 0.239 and 0.07 respectively) (Table 6).

**Table (6):** Correlation between MIBI parameters, age, TSH, and nodule size in 21 patients with thyroid nodules.

Variable	Age		TSH		Nodule size	
	r	P	r	P	r	P
WOI-P	0.111	0.636	0.182	0.430	0.202	0.393
WOI-S	0.110	0.350	-0.10	0.643	-0.193	0.414
RI-P	0.215	0.976	-0.11	0.631	-0.276	0.239
RI-S	0.007	0.633	0.336	0.136	-0.413	0.07
Nodule size	-0.264	0.616	-0.140	0.555		

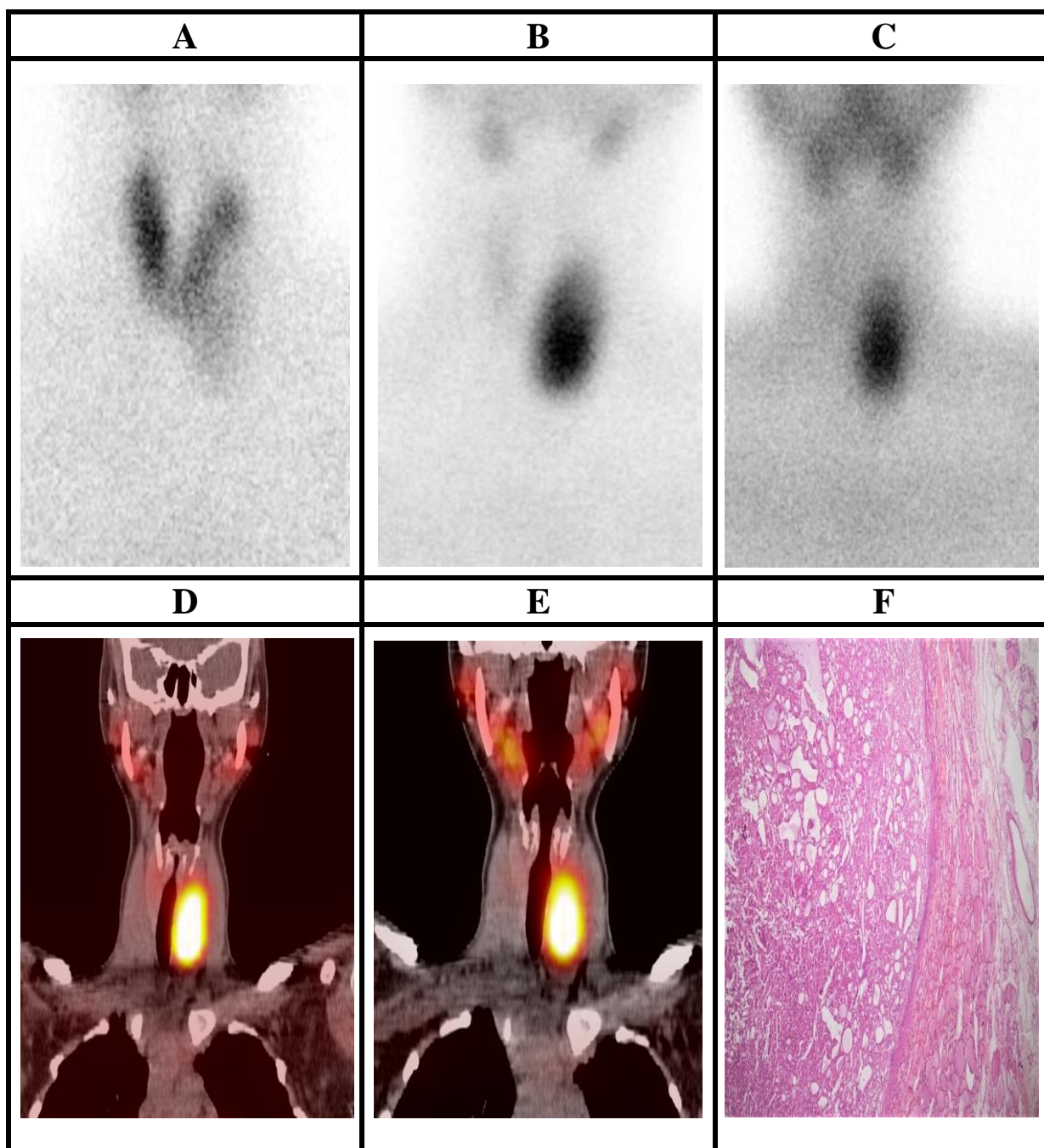


**Figure (1):** A 23-years-old female with a solitary nodule located in the left thyroid lobe corresponding to the US nodule and cytological reading of follicular neoplasm. (A)  $^{99m}\text{Tc}$ -pertechnetate thyroid scintigraphy showed a hypofunctioning nodule in the left lobe (score 1). (B&C)  $^{99m}\text{Tc}$ -MIBI planar images obtained at 30 (early, score 3) and 90 (delayed, score 3) minutes after tracer administration. (D&E) Early and delayed SPECT/CT images: washout pattern consistent with increased uptake (tracer retention). (F) Final histopathological diagnosis of follicular adenoma with evident intact, well defined capsule.

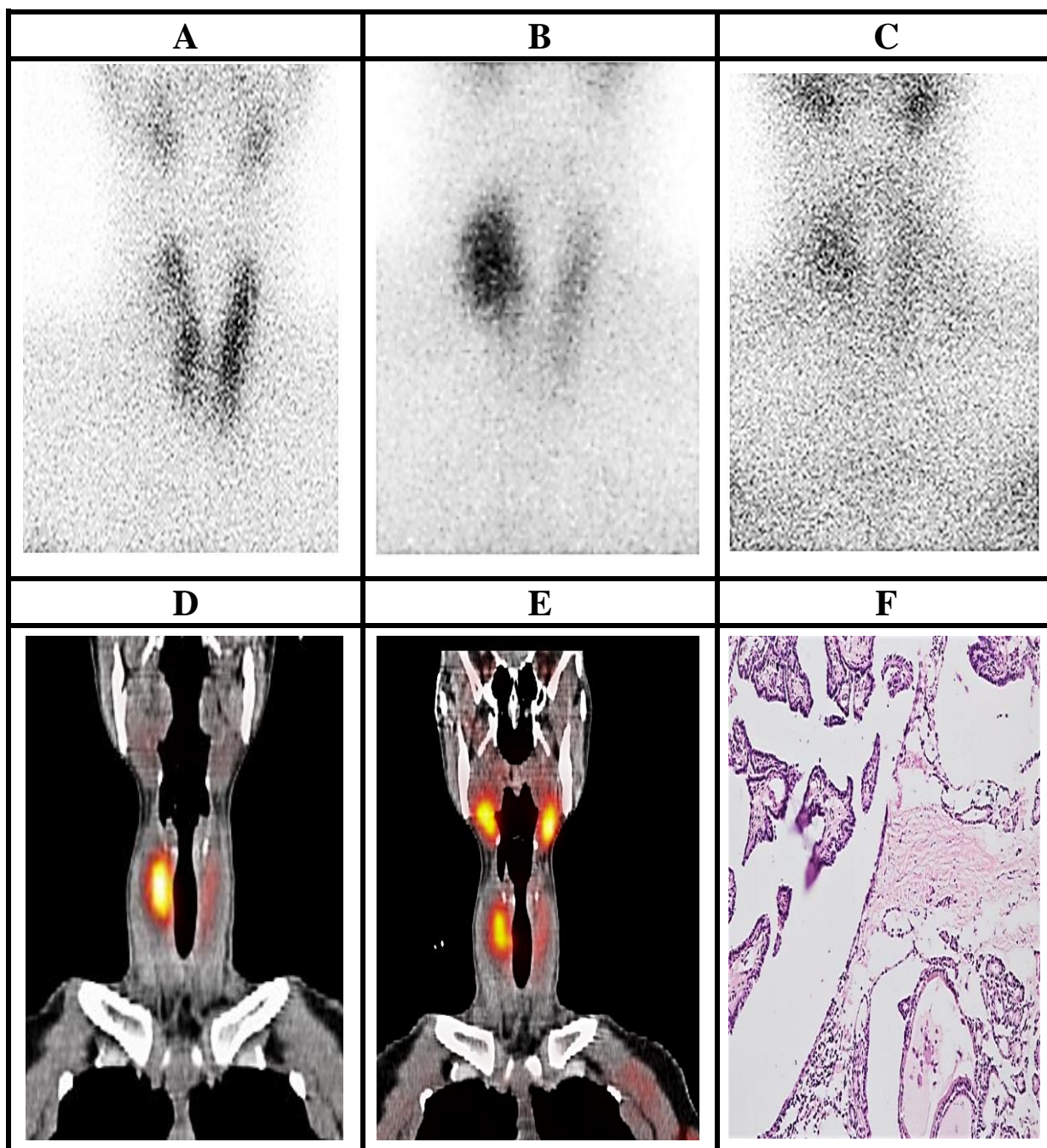


**Figure (2):** A 25-years-old female with a solitary nodule located in the right thyroid lobe corresponding to the US nodule and cytological reading of follicular neoplasm. (A)  $^{99m}\text{Tc}$ -pertechnetate thyroid scintigraphy showed a hypo functioning nodule in the middle third of the right lobe (score 0).

(B&C)  $^{99m}\text{Tc}$ -MIBI planar images obtained at 30 (early, score 3) and 90 (delayed, score 2) minutes after tracer administration respectively. (D&E) Early and delayed SPECT/CT images: washout pattern consistent with constant uptake. (F) Final histopathological diagnosis of follicular variant of papillary thyroid carcinoma.

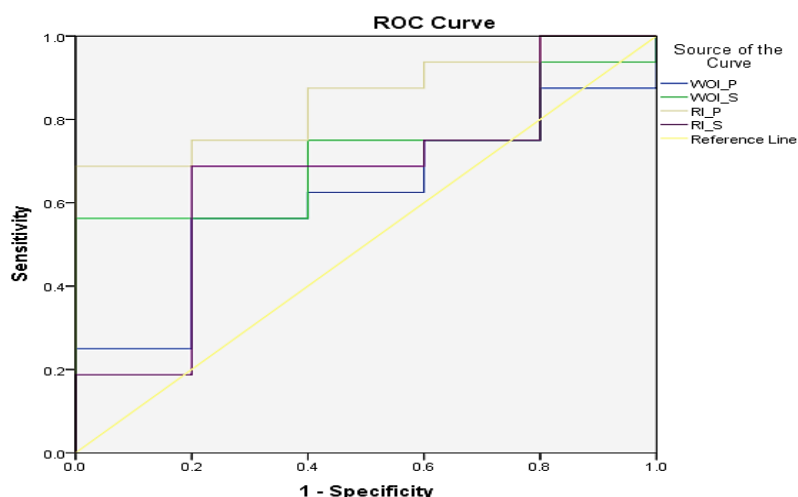


**Figure (3):** ROC analysis of quantitative MIBI parameters.

## DISCUSSION:

Diagnostic approach of the thyroid nodules includes laboratory tests and US as well as thyroid scintigraphy to rule out autonomously functioning nodules that are considered as benign, with a high degree of certainty<sup>(3)</sup>.

In 2015 American Thyroid Association (ATA) guidelines for the management of patients with thyroid nodules and differentiated thyroid cancer considered the thyroid US to have a central role in the management of thyroid nodules and recommended that biopsy should be done based on the sonographic pattern<sup>(1,16)</sup>.

FNAC is a simple, cost-effective test for cancer diagnosis, and its use has greatly decreased the number of unnecessary thyroid surgeries<sup>(17)</sup>.

However, the most important obstacle of FNAB is the lack of sensitivity in the characterization of follicular neoplasms because of its inability to detect capsular/vascular invasion of the tumor. Furthermore, diagnosis by FNAC may be a challenge in cases with follicular variants of papillary carcinoma, where the classic diagnostic cytological criteria of papillary carcinoma are lacking (i.e. papillary structures), as well as in patients with a hyper cellular pattern of micro follicular goiter<sup>(4)</sup>.

Several publications reported the diagnostic value of MIBI-scintigraphy for the evaluation of thyroid nodule based on the degree of uptake of MIBI by the nodule and/or the change in this uptake over time<sup>(18)</sup>.

In a meta-analysis, the pooled sensitivity and specificity of MIBI scan in detecting malignant thyroid nodules were 85.1 % and 45.7 % respectively, in another meta-analysis and systemic review the pooled sensitivity was 87% and specificity of 78 % (19, 20), keeping with these results we reported 80 % sensitivity and 75% specificity for planar imaging versus sensitivity of 80 % and 81.2% specificity for SPECT/CT imaging.

SPECT acquisition combined with iterative reconstruction proved superior to planar imaging alone, especially in differentiating isointense nodules from those with either decreased or increased MIBI uptake. Therefore, SPECT had an adequately high NPV and allowed detection of most carcinomas even less than 1 cm in diameter (21). In our cohort the specificity, PPV, and NPV of the MIBI SPECT/CT scanning were higher than those of planar imaging.

It is important to know that MIBI has a high negative predictive value up to 100% with a mean of more than 97% (18), our study revealed a relatively lower NPV of 92.3 %, this could be attributed to the inclusion of isofunctioning as well as hypofunctioning nodules on <sup>99m</sup>Tc-scintigraphy in the present study. *Giovanella et al.*, found that MIBI scintigraphy had NPV of 100% in

ruling out malignant thyroid nodules if the nodules were cold on <sup>99m</sup>Tc-scintigraphy and negative on MIBI imaging (22).

The positive predictive value for MIBI scintigraphy ranges from <10% up to 60% (23, 24), we encountered a value of 50% in our study population, in contrast, *Theissen et al.*, found a lower value of 20% (21), the wide range of values may be attributed to the different prevalence rate of thyroid malignancy in the studied population.

The main disadvantage of <sup>99m</sup>Tc-MIBI is that an increased uptake does not necessarily means malignancy, it was found that 23% of nodules with positive MIBI uptake finally diagnosed as benign lesions (false positive) (25).

In our cohort, 4 (~19%) false positive results by planar imaging were found in whom the pathology was consistent with typical follicular adenoma, similar figure was reported by *Foldes et al.* (26). SPECT/CT decreased the number of false positive to 3 cases by detecting washout in one nodule with isointense uptake.

Although false-negative results are rarely reported in literature, two patients with anaplastic /undifferentiated carcinoma were falsely interpreted as negative results by *Foldes et al.* and *Kresnik et al.* (26, 27).

Additionally *Theissen et al.* and *Sathekge et al.*, had reported small number of patients with follicular and papillary carcinomas that was falsely interpreted as negative for malignancy<sup>(21, 28)</sup>.

In line with the previously mentioned studies we encountered one patient with minimally invasive follicular carcinoma whose result was interpreted as negative in both planar and SPECT/CT imaging.

*Theissen et al.*, attributed his false negative results to the difficulties for MIBI scanning in case of goiters with different pathologies; where the hypofunctioning nodule was adjacent to an autonomous nodule or due to false positive histological result in assessing hyper cellular or heterogeneous adenomas<sup>(21)</sup>.

On the other hand, *Boi* and *coauthors* investigated Hurthle cell neoplasms and attributed the false negative MIBI results to the small tumor size or to image misinterpretation<sup>(13)</sup>.

Degenerative nodules rarely express MIBI over-accumulation; accordingly our false negative result can be explained (nodule size of 2.5 cm with a well-defined margins

and degenerative changes was detected in the SPECT/CT images), similar explanation was done by *Mezosi et al.*,<sup>(29)</sup>.

In our study, different levels of activity were observed in the early and delayed MIBI scans, when a nodule with score 2 or 3 in delayed images was considered as malignant lesion, the scan provided 100% sensitivity and NPV of 100% in discriminating benign from malignant nodules, these figures were in line with *Riazi et al.*,<sup>(30)</sup>.

A negative MIBI scan indicated a benign etiology in most patients (92.3 %), therefore when the MIBI scan is negative surgery could be avoided. Positive MIBI scans were actually indeterminate or non-diagnostic as most patients with a positive MIBI scan had benign nodules.

*Schenke et al.*, reported inter-reader variability of 0.76 and 0.80 for planar and SPECT MIBI images respectively<sup>(31)</sup>, we found higher values for both planar and SPECT (1 for early planar , 0.78 for delayed planar and 1 for SPECT) images, additionally we found a value of 0.90 for thyroid scan.



*Saggiorato* and *coauthors* were the first to investigate the possible role of quantitative analysis (RI method) for improving diagnostic performance of MIBI scanning in patients with thyroid nodules <sup>(12)</sup>, then other authors had introduced the so called WOI method <sup>(22, 32)</sup>.

*Campenni et al.*, for the first time compared the two quantitative methods and concluded that calculation of WOI is highly accurate in the differential diagnosis of nodules with indeterminate cytology results <sup>(3)</sup>.

In contrast to *Saggiorato et al.*, who found no significant differences in the RI between malignant and benign thyroid nodules <sup>(12)</sup>, we found that the median RI-P of benign nodules was significantly lower than that of malignant ones ( $31.6 \pm 63.2$  vs.  $42.9 \pm 41$ ,  $P=0.024$ ).

In a study carried out by *Riazi et al.*, they found that the area under the ROC curve for the RI was 0.826, and the optimal cutoff point for RI was 0.16; giving a sensitivity and a specificity of 80 and 79% respectively <sup>(30)</sup>. *Erdil et al.*, used a cut-off point of 2 for MIBI RI, giving 95.2% sensitivity and 89.4% specificity <sup>(33)</sup>. In the current study the AUC for RI-P was 0.850; considering the best cut-off point as -114; it gave a sensitivity, specificity, NPV,

and PVV of 100 % for all, the different cut-off point can be explained by different instrumentation used, together with being an operator dependent.

In the previous studies, the overall sensitivity and specificity of WOI in identifying patients with malignant lesions were 100% and 90%, respectively <sup>(22, 32)</sup>. In the current work, a lower sensitivity of about 93.8% and a higher specificity of 100% were obtained by using the WOI method for both planar and SPECT/CT images, while identical high sensitivity and specificity (100% for both) were attained when using RI-P.

To our knowledge, this is the first study to conduct semi quantitative analysis for both planar and SPECT/CT images and to compare the results with the nodule characteristics. We found insignificant positive correlation between nodule size and WOI-P ( $r=0.202$ ,  $p=0.393$ ), while insignificant negative correlation was found between it and each of TSH, WOI-S, RI-P and RI-S ( $r=0.277$ ,  $-0.140$ ,  $-0.193$ ,  $-0.276$ , and  $-0.413$  with  $P=0.616$ ,  $0.555$ ,  $0.414$ ,  $0.239$ , and  $0.07$  respectively).

In contrast to *Saggiorato et al.*, who found no correlation between nodule size and RI value ( $r = -0.098$ ,  $P = 0,486$ ) <sup>(12)</sup>.

### **Limitations of the study:**

The relatively small sample size and the single center experience were the limitation of our study, additionally the semi-quantitative analysis is partially an operator-dependent technique, especially with regard to the definition of the VOIs. Furthermore, this technique is dependent on the instrumentation used. Therefore, each center needs to optimize a special protocol and to define its own cut-off values.

On the contrary, the advantages of the current study include the use of both planar and SPECT/CT imaging techniques with semi quantitative parameters for both methods and the use of visual scoring system to enhance sensitivity.

### **REFERENCES:**

1. **Haugen BR, Alexander EK, Bible KC, et al.,** American Thyroid Association management guidelines for adult patients with thyroid nodules and differentiated thyroid cancer: the American Thyroid Association guidelines task force on thyroid nodules and differentiated thyroid cancer. *Thyroid*, 26 (1):1-133; 2016.
2. **Hegedüs L.** The thyroid nodule. *New England Journal of Medicine*, 351 (17):1764-71; 2004.

### **CONCLUSIONS:**

The visual scoring system yields a high sensitivity and NPV yet has a low specificity. Addition of SPECT/CT improves the diagnostic accuracy of the washout pattern in the delayed images. Furthermore, semi-quantitative analysis using WOI and RI methods is a useful tool which improved the diagnostic performance of MIBI scintigraphy in evaluating thyroid nodules with a cytologic diagnosis of follicular neoplasm, yet RI-P semi-quantitative parameter was the only significant predictor index for malignancy. We recommended a multicenter study with larger sample size over a long duration to validate the importance of our results.

3. **Campennì A, Siracusa M, Ruggeri R, et al.,** Differentiating malignant from benign thyroid nodules with indeterminate cytology by 99m Tc-MIBI scan: a new quantitative method for improving diagnostic accuracy. *Scientific reports*, 7 (1):1-6; 2017.
4. **Trimboli P and Durante C.** Ultrasound risk stratification systems for thyroid nodule: between lights and shadows, we are moving towards a new era. *Endocrine*, 69:1-4; 2020.

5. **Wong C, Liu X, Lang B.** Cost-effectiveness of fine-needle aspiration cytology (FNAC) and watchful observation for incidental thyroid nodules. *Journal of endocrinological investigation*, 43 (11):1645-54; 2020.
6. **Malheiros DC, Canberk S, Poller D, et al.** Thyroid FNAC: Causes of false-positive results. *Cytopathology*, 29 (5):407-17; 2018.
7. **Zhu Y, Song Y, Xu G, et al.** Causes of misdiagnoses by thyroid fine-needle aspiration cytology (FNAC): our experience and a systematic review. *Diagnostic pathology*, 15 (1):1-8; 2020.
8. **Suster S.** Thyroid tumors with a follicular growth pattern: problems in differential diagnosis. *Archives of pathology & laboratory medicine*, 130 (7):984-8; 2006.
9. **Chehboun A, Foudil D, Naili Q, et al.** Technetium-99m MIBI Scintigraphy Contribution in the Assessment of Cold Thyroid Nodule. *EANM*, OP-113; 2019.
10. **Giovanella L, Ceriani L, Treglia G.** Role of isotope scan, including positron emission tomography/computed tomography, in nodular goitre. *Best Practice & Research Clinical Endocrinology & Metabolism*, 28 (4):507-18; 2014.
11. **Rager O, Radojewski P, Dumont RA, et al.** Radioisotope imaging for discriminating benign from malignant cytologically indeterminate thyroid nodules. *Gland surgery*, 8 (2):S118; 2019.
12. **Saggiorato E, Angusti T, Rosas R, et al.** 99mTc-MIBI Imaging in the presurgical characterization of thyroid follicular neoplasms: relationship to multidrug resistance protein expression. *Journal of Nuclear Medicine*, 50 (11):1785-93; 2009.
13. **Boi F, Lai M, Deias C, et al.** The usefulness of 99mTc-SestaMIBI scan in the diagnostic evaluation of thyroid nodules with oncocyctic cytology. *European journal of endocrinology*, 149(6):493-8; 2003.
14. **Barbara A. Crothers, Michael R. Henry, Pinar Firat, et al.** Nondiagnostic/Unsatisfactory. In: Ali SZ, Cibas ES, editors. *The Bethesda System for Reporting Thyroid Cytopathology: Definitions, Criteria, and Explanatory Notes*. 2nd ed: Springer, P. 7-18; 2018.
15. **Michael R. Henry, William H. Westra, Jeffrey F. Krane, et al.** Follicular Neoplasm/ Suspicious for a Follicular Neoplasm. In: Ali SZ, Cibas ES, editors. *The Bethesda System for Reporting Thyroid Cytopathology: Definitions, Criteria, and Explanatory Notes*. 2nd ed: Springer, p. 71-80; 2018.

- 16. Valderrabano P, McGettigan MJ, Lam CA, et al.,** Thyroid nodules with indeterminate cytology: utility of the American Thyroid Association sonographic patterns for cancer risk stratification. *Thyroid*, 28 (8):1004-12; 2018.
- 17. Cibas ES and Ali SZ.** The Bethesda system for reporting thyroid cytopathology. *Thyroid*, 19 (11):1159-65; 2009.
- 18. Yordanova A, Mahjoob S, Lingohr P, et al.,** Diagnostic accuracy of [99mTc] Tc-Sestamibi in the assessment of thyroid nodules. *Oncotarget*, 8 (55):94681; 2017.
- 19. Treglia G, Caldarella C, Saggiorato E, et al.,** Diagnostic performance of 99m Tc-MIBI scan in predicting the malignancy of thyroid nodules: a meta-analysis. *Springer*, 44: 70-78; 2013.
- 20. Kim S-J, Lee S-W, Jeong SY, et al.,** Diagnostic performance of technetium-99m methoxy-isobutyl-isonitrile for differentiation of malignant thyroid nodules: a systematic review and meta-analysis. *Thyroid*, 28 (10):1339-48; 2018.
- 21. Theissen P, Schmidt M, Ivanova T, et al.,** MIBI scintigraphy in hypofunctioning thyroid nodules. *Nuklearmedizin*, 48(04):144-52; 2009.
- 22. Campennì A, Giovanella L, Siracusa M, et al.,** 99mTc-methoxy-isobutyl-isonitrile scintigraphy is a useful tool for assessing the risk of malignancy in thyroid nodules with indeterminate fine-needle cytology. *Thyroid*, 26 (8):1101-9; 2016.
- 23. Hurtado-López LM, Arellano-Montaña S, Torres-Acosta EM, et al.,** Combined use of fine-needle aspiration biopsy, MIBI scans and frozen section biopsy offers the best diagnostic accuracy in the assessment of the hypofunctioning solitary thyroid nodule. *European journal of nuclear medicine and molecular imaging*, 31 (9):1273-9; 2004.
- 24. Alonso O, Mut F, Lago G, et al.,** 99Tc (m)-MIBI scanning of the thyroid gland in patients with markedly decreased pertechnetate uptake. *Nuclear medicine communications*, 19 (3):257-61; 1998.
- 25. Schmidt M.** Tc-99m-MIBI for Thyroid Imaging. *99mTc-Sestamibi: Springer*, P. 133-58; 2012.
- 26. Földes I, Lévy A, Stotz G.** Comparative scanning of thyroid nodules with technetium-99m pertechnetate and technetium-99m methoxyisobutylisonitrile. *European journal of nuclear medicine*, 20 (4):330-3; 1993.

- 27. Kresnik E, Gallowitsch H-J, Mikosch P, et al.**, Technetium-99m-MIBI scintigraphy of thyroid nodules in an endemic goiter area. *Journal of nuclear medicine*, 38 (1):62-5; 1997.
- 28. Sathekge MM, Mageza RB, Muthuphei MN, et al.**, Evaluation of thyroid nodules with technetium-99m MIBI and technetium-99m pertechnetate. *Head & neck*, 23 (4):305-10; 2001.
- 29. Mezosi E, Bajnok L, Gyory F, et al.**, The role of technetium-99m methoxyisobutylisonitrile scintigraphy in the differential diagnosis of cold thyroid nodules. *European journal of nuclear medicine*, 26 (8):798-803;1999.
- 30. Riazi A, Kalantarhormozi M, Nabipour I, et al.**, Technetium-99m methoxyisobutylisonitrile scintigraphy in the assessment of cold thyroid nodules: is it time to change the approach to the management of cold thyroid nodules? *Nuclear Medicine Communications*, 35 (1):51-7; 2014.
- 31. Schenke S, Klett R, Acker P, et al.**, Interobserver Agreement of Planar and SPECT Tc99m-MIBI Scintigraphy for the Assessment of Hypofunctioning Thyroid Nodules. *Nuklearmedizin*, 58 (03):258-64; 2019.
- 32. Giovanella L, Campenni A, Treglia G, et al.**, Molecular imaging with 99m Tc-MIBI and molecular testing for mutations in differentiating benign from malignant follicular neoplasm: a prospective comparison. *European journal of nuclear medicine and molecular imaging*, 43 (6):1018-26; 2016.
- 33. Erdil TY, Özker K, Kabasakal L, et al.**, Correlation of technetium-99m MIBI and thallium-201 retention in solitary cold thyroid nodules with postoperative histopathology. *European journal of nuclear medicine*, 27 (6):713-20; 2000.